Optimization of Artificial Diffusion Stabilization Techniques and Corresponding Mesh density Distribution in Drift Dominated Transport of Diluted Species

Jouya Jadidian[*1], Markus Zahn[1], Nils Lavesson[2], Ola Widlund[2] and Karl Borg[2]
[1] Massachusetts Institute of Technology, MA 02139, USA
[2] ABB Corporate Research, Västerås, SE 72178, Sweden
*Corresponding author: 77 Massachusetts Ave., Room 10-061, jouya@mit.edu

Abstract: This paper presents an optimized combination of artificial diffusion techniques to stabilize a drift dominated streamer discharge model which includes COMSOL Multiphysics' Transport of Diluted Species modules for positive ion, negative ion, and electron charge densities, coupled through the Electrostatic module. A Thermal Conduction and Convection module is responsible for the heat transfer in the model. Optimal 2D axisymmetric and 3D mesh schemes are also introduced to effectively solve the numerical problem. Several combinations of streamline diffusions and Crosswind diffusion with different tuning parameters are applied to the charge continuity and the thermal equations with different mesh element size distributions to determine the ideal approach.

Keywords: Convection and diffusion, artificial diffusion, streamer, liquid dielectrics, transformer oil

1. Introduction

The performance of different consistent stabilization techniques is investigated in a three-carrier streamer continuum model, which is utilized to account for the charge generation, recombination, and transport mechanisms in a liquid dielectric. The governing equations that contain the physics to model streamer development in liquids are based on the drift-dominated charge continuity equations for positive ion, negative ion, and electron charge densities, coupled through the Gauss' law. The thermal diffusion equation is included to model temperature variations and gas formation in the liquid. The mobility dependencies on electric field intensity and temperature have been taken into account. The model is implemented in both 2D axisymmetric and 3D geometries. Figure 1 shows the experimental view of the discharge chamber.

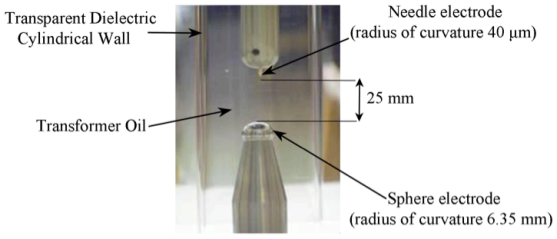

Figure 1. Needle-sphere electrode geometry used for streamer simulation purposes as described in IEC 60897 standard [1]. The electrodes are 25 mm apart and the radii of curvature of the needle and sphere electrodes are 40 μm and 6.35 mm, respectively [2].

Several Streamline Diffusions (SD), such as anisotropic [3], Upwind Petrov-Galerkin, and Galerkin least-squares [3,4], along with Crosswind (CWD) diffusion [3-5] are applied to stabilize the charge continuity and thermal diffusion equations. These techniques are compared when used either alone or in combination, with different tuning parameters. The streamer modeling results show that the artificial diffusion techniques can save great amounts of simulation time and computational capacity if used appropriately. In particular, COMSOL Multiphysics 3.5a SD techniques are quite effective in the charge transport problem and cannot be avoided due to convergence issues. In COMSOL Multiphysics 4.3, however, the CWD is much more robust and can replace the SD. Since the local element size can be used in determining the CWD tuning parameter, the 3D problem can converge much easier and faster using CWD in version 4.3 or 4.2a. In terms of accuracy, the artificial diffusion tuning parameters must be minimized if possible. In other words, there is usually a tradeoff between reducing the tuning parameters and required mesh size to reach the convergence and accurate results. The simulation results, simulation times, and the required mesh density distributions for different applied artificial diffusion techniques are presented.

To eliminate nonphysical instabilities, we have tested several dense mesh schemes. It has been shown that only refining the mesh around the needle tip is not sufficient to solve the problem. The distribution of mesh element size in the volume around the needle is rather essential, meaning that a smoothly growing element size does not result in nonphysical growing instabilities as opposed to a sudden change of the element size over a boundary.

2. Use of COMSOL Multiphysics

The governing equations are based on the drift-dominated charge continuity, Eqs. (1)-(3), for positive ion (ρ_p), negative ion (ρ_n) and electron (ρ_e) charge densities, coupled through Gauss' law, Eq. (4). The thermal diffusion, Eq. (5), is included to model temperature variations (T) in oil. The negative ion and electron charge densities in governing equations are both negative quantities [6-10].

$$\frac{\partial \rho_p}{\partial t} + \nabla \cdot (\rho_p \mu_p \bar{E}) = G_M(|\bar{E}|) + \frac{\rho_p \rho_e R_{pe}}{q} + \frac{\rho_p \rho_n R_{pn}}{q} \quad (1)$$

$$\frac{\partial \rho_n}{\partial t} - \nabla \cdot (\rho_n \mu_n \bar{E}) = \frac{\rho_e}{\tau_a} - \frac{\rho_p \rho_n R_{pn}}{q} \quad (2)$$

$$\frac{\partial \rho_e}{\partial t} - \nabla \cdot (\rho_e \mu_e \bar{E}) = -G_M(|\bar{E}|) - \frac{\rho_p \rho_e R_{pe}}{q} - \frac{\rho_e}{\tau_a} \quad (3)$$

$$\nabla \cdot (\varepsilon \bar{E}) = \rho_p + \rho_n + \rho_e \quad (4)$$

$$\frac{\partial T}{\partial t} + v \cdot \nabla T = \frac{1}{\rho_l c_v}(k_T \nabla^2 T + \bar{E} \cdot \bar{J}) \quad (5)$$

where v, ε, k_T, c_v, and ρ_l are the oil's velocity, permittivity (2.2 ε_0), thermal conductivity, specific heat, and mass density, respectively. Representative values for transformer oil are listed in Table 1. In the microsecond time scales of interest for streamer formation, the oil velocity is negligible such that v=0. In addition, q is the magnitude of electronic charge and E is the local electric field. The parameters μ_p, μ_n, and μ_e are the mobilities of the positive ions, negative ions and electrons respectively. The ion-ion recombination rate, R_{pn} is obtained from the Langevin-Debye relationship [6-8],

$$R_{pn} = q(\mu_n + \mu_p)/\varepsilon \quad (6)$$

The ion-electron recombination rate, R_{pe}, is assumed equal to ion-ion recombination rate, since using the Langevin-Debye relationship for the ion-electron recombination rate leads to some overestimation [6,7]. In addition to re-combination, electrons also combine with neutral molecules to form negative ions. This process is described as an electron attachment time constant, τ_a = 200 ns [7,8]. The generation and recombination terms play a key role in describing streamer dynamics. The field ionization charge density rate source term, G_M, is modeled using the Zener model of electron tunneling in solids that is improved by Density Functional Theory (DFT) [8,11]:

$$G_M(|\bar{E}|) = \frac{q^2 n_0 a |\bar{E}|}{h} \exp\left(-\frac{\pi^2 m^* a}{qh^2}\left(\frac{\Delta}{\sqrt{|\bar{E}|}} - \gamma\right)^2\right) \quad (7)$$

All parameter definitions and values are given in Table 1. Application of the generation term in the form of Eq. (7) in Eqs. (1) and (3) enables the model to describe the negative and positive streamers formed by high voltages [8].

The needle electrode potential is defined by subtracting two exponential functions that create the standard lightning impulse voltage according to IEC 600060-1 [12] as

$$V_{impulse} = KV_0\,(e^{-\frac{t}{\tau_1}} - e^{-\frac{t}{\tau_2}}) \quad (8)$$

where K is a non-dimensional compensation factor to keep the peak amplitude of the impulse approximately equal to V_0, since in general, the maximum value of two subtracting exponential functions in Eq. (8) is not necessarily 1. The potential of the sphere electrode is set to the ground. The top, bottom, and side insulating walls of the breakdown chamber (transparent cylindrical dielectric wall in Fig. 1) have been assigned to have zero normal displacement field components ($\vec{n} \cdot \vec{D} = 0$). This boundary condition acts as a zero surface charge equation on the wall that also guarantees cylindrical symmetry. The boundary conditions for the charge transport continuity equations at electrodes are set to "convective fluxes" for all species [8], while insulating wall boundaries are assigned to have no flux of any species. All boundaries are set to zero normal thermal diffusive flux (i.e., $\vec{n}.\vec{\nabla}T = 0$) making the approximation that the system is adiabatic on the timescales of interest [7,8].

Table1: Physical parameters used in the model [7,8]

Symbol	Parameter	Value
n_0	Number density of ionizable species	1×10^{23} m^{-3}
a	Molecular separation distance	3.0×10^{-10} m
m^*	Effective electron mass	$0.1\times m_e = 9.1\times10^{-32}$ kg
A, γ	Ionization potential function parameters	1.36×10^{-18} J, 1.118×10^{-23} Jcm$^{1/2}$V$^{-1/2}$
R_{pn},R_{pe}	Ion-ion and ion-electron recombination rates	1.64×10^{-17} m^{3}s^{-1}
μ_p,μ_n	Positive and negative ion mobilities	10^{-9} m^{2}V^{-1}s^{-1}
μ_e	Electron mobility	10^{-4} m^{2}V^{-1}s^{-1}
c_v	Specific heat	1.7×10^3 Jkg^{-1}K^{-1}
ρ_l	Oil mass density	880 kgm^{-3}
k_T	Thermal Conductivity	0.13 Wm^{-1}K^{-1}
q	Electronic charge	1.602×10^{-19} C
h	Planck's constant	6.626068×10^{-34} m^{2}kgs^{-1}

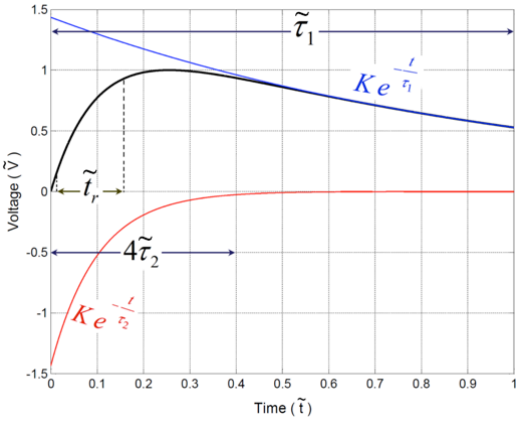

Figure 2. IEC 60060 lightning impulse voltage (non-dimensional, $\tilde{V} = V / V_0$) with rise-time t_r (10% to 90% of peak voltage) versus non-dimensional time, $\tilde{t} = t / \tau_1$ [12].

We have solved the conservative form of the general convection and diffusion equations in COMSOL Multiphysics. Two direct solvers, MUMPS and PARDISO are employed separately to solve the streamer model. These solvers are well known to be robust and memory efficient tools in parallel high performance computing [3,4]. Solutions of these solvers are in excellent agreement for ~10^6 degrees of freedom. These direct solvers have proved to be more accurate compared to the iterative solvers, although they are computationally more expensive. Since the present model contains nonsymmetrical matrices and nonlinear equations, combinations of direct and iterative solvers have been applied to speed up the solution. Three computer machines with a total 36 threads (~3.4 GHz) and 188 GB are used in parallel to solve Eqs. (1)-(8). A typical simulation takes ~50 hours to finish with 10^6 degree of freedom.

3. Optimized combination of stabilization techniques

Diffusion of the charged species is assumed negligible in Eqs. (1-3). Numerical solutions of the charge continuity equations usually include spatial instabilities rather than expected smooth solutions [3-5]. These spurious oscillations can be avoided by using nonlinear CWD in addition to different types of SDs such as anisotropic, compensated streamline upwind Petrov-Galerkin (SUPG) and Galerkin least-square methods, to stabilize the charge continuity equations [3,4]. It has been shown in [5], that CWD is more stable than other over-diffusive discontinuity-capturing techniques and leads to better numerical behavior, although it is computationally expensive due to its non-linear nature [3,4]. On the other hand, SD techniques effectively stabilize the system and accelerate the solution. We have applied minimal SD and CWD at the same time to optimally stabilize the numerical solution [6,18]. Minimal artificial diffusion techniques are tuned to balance a tradeoff between removing nonphysical local oscillations (due to SD) and excessively smooth results just next to the walls (due to CWD) [8].

Including CWD effectively damps oscillations in the charge number densities and prevents them from becoming negative which is nonphysical. It also increases the streamer diameter and decreases the streamer velocity and the maximum electric field ahead of the streamer compared to the results obtained using SD only. This is reasonable if we remember that CWD adds some artificial diffusion terms orthogonal to the flow of species to stabilize the numerical solution [3,4]. The CWD also provides extra diffusion in the region of sharp gradients.

In spite of COMSOL 3.5a, SD is sometimes not enough to converge the streamer model in COMSOL 4.2a and 4.3, which makes it harder to compare results of the SD only cases. In

addition, COMSOL 4.3 employs only one SD type without any tuning parameters. COMSOL recommends in [4] that "Both artificial diffusions should be selected for optimal performance."

The CWD method specifies the smallest allowable concentration change across an element. As the concentration gradient appears in the denominator in the equations describing CWD, the gradient ensures that unreasonable values do not occur in regions with small to negligible concentration changes [4].

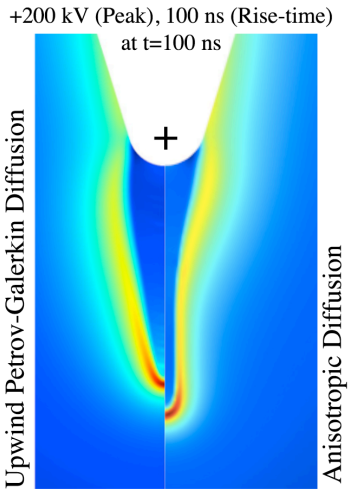

Figure 3. Different streamer propagation mechanisms under two different artificial diffusions: electric field magnitude distribution solved by (left): upwind Petrov-Galerkin diffusion and (right): anisotropic diffusion. The applied voltage peak magnitude to the positive needle is 200 kV and the rise-time is 100 ns.

4. Mesh element size distribution

If the applied voltage is steep enough to form an initial charge volume larger than 0.2 mm diameter, off-axis branching is likely to happen in 2D axisymmetric geometry. Based on experimental observations, the cone-shaped instability (Fig. 4) is nonphysical and assumed to be a consequence of element size distribution especially in the vicinity of the needle electrode. Such off-axis deflections of the streamer head will not disappear even if we add either excessive CWD or large inconsistent isotropic diffusion terms to the equations. The reason for branching phenomena in our streamer model is the nature of the SD concept. In fact, this artificial stabilizer adds greater diffusion terms at those points where electric field lines are denser (convergent or divergent). As described earlier, the SD term is in the direction that strengthens the particle velocity in the particle motion streamline direction. Since electrons are very mobile, the SD based model is vulnerable to any spatial noise. This is even worse in our model since such excessive diffusions can accumulate the charge off the axis of symmetry which itself increases the electric field in those directions and consequently generates more charge based on the Zener molecular ionization equation. Such off-axis branches disappear if we remove SD. It has been known that the charge conservation equations never converge without a consistent stabilization method. Thus the only option to prove that these branches form because of SD is to use CWD. We have not observed any off-axis branching formed when we apply only CWD. However, removing SD decreases the streamer velocity, which does not agree with experimental observations. This makes it an obligation for us to deal with SD sensitivities. To overcome these off-axis instabilities we tested several dense mesh distributions in the needle-sphere geometry. It has already been proven that only refining the mesh around the needle tip cannot solve the problem as for example shown in Fig. 4 for a box with an excessively dense mesh (maximum mesh element of 0.5 μm).

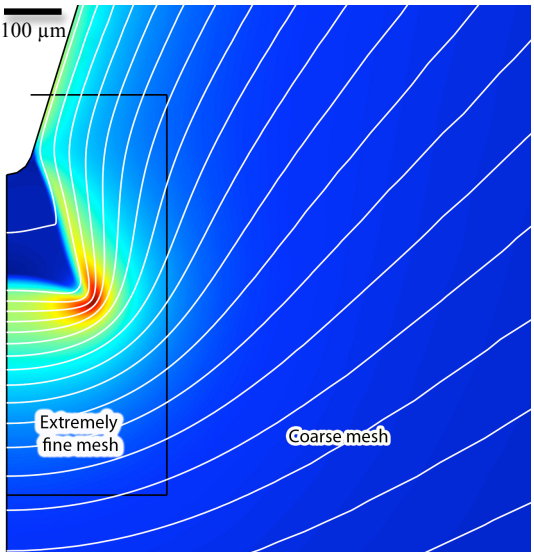

Figure 4. Off-axis branching in a streamer formed by a positive impulse with 200 kV and 1 ns rise-time still appears even with an extremely fine mesh around the needle (colors and white lines depict electric field and equipotential lines, respectively).

Figure 5 shows the simulation results of a smoothly distributed element size. In this mesh scheme, we have successfully removed off-axis instability; instead, an axial high-speed streamer branch evolves from the initially ionized volume. In this case, we have employed an extremely dense mesh on the axis of symmetry and a larger rectangular dense mesh area around the needle tip (maximum element size of 2 µm) while the total number of elements is almost the same as Fig. 4. The main difference between these two cases is that we have avoided any jump in element size in the critical area (Fig. 5). The position and dimensions of this critical area are mainly determined by the applied voltage waveform and the molecular properties of bulk oil (such as the ionization potential, number of ionizable species, etc.). For a +200 kV, 100 ns impulse, the critical zone is up to one millimeter from the needle.

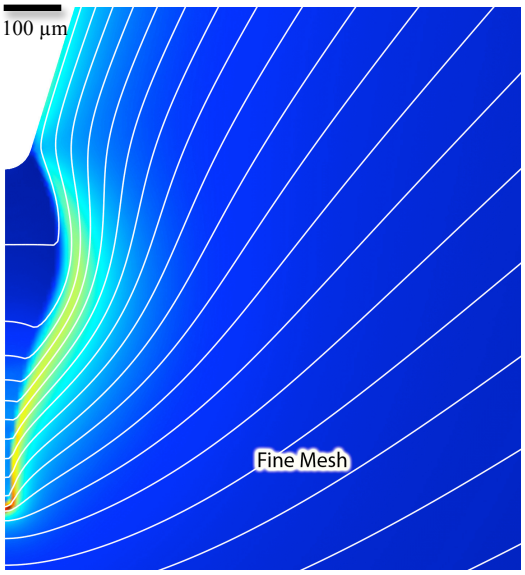

Figure 5. Off-axis branching in a positive streamer formed by a positive impulse with 200 kV and 1 ns rise-time disappears even with a fine mesh over a larger box around the needle (colors and white lines depict electric field and equipotential lines, respectively).

Increasing the mesh density in the vicinity of the needle electrode generally decreases the streamer velocity. If we refine the mesh more smoothly over the space around the needle (left side of Fig. 6), the result is more consistent to the physical expectations compared with an extremely dense mesh over a smaller rectangle around the needle tip (right side of Fig. 6). For instance, the number of streamlines deflected in the off-axis direction for the left hand side picture of Fig. 6 is increased and consequently a deflection is formed on the streamer surface. We have also confirmed this idea with adapted mesh feature of COMSOL 4.3. The left side of Fig. 6 has been obtained by activating the adapted mesh feature of COMSOL 4.3 which takes about 10 times longer simulation time to converge. The importance of this comparison is that the conclusion of last paragraph of section (1-c) is consistent with the COMSOL 4.3 adapted meshing policy that uses smoother mesh element size distribution (Fig. 6 left side).

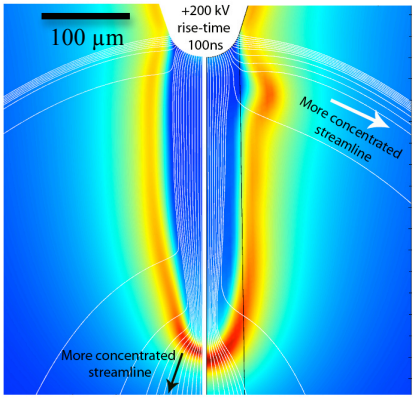

Figure 6. Electric field magnitude (color) and streamlines (white lines) for two different mesh element size distributions under a positively applied voltage (200 kV peak and 100 ns rise-time at time 85 ns). The two simulations are separately computed with the left side plot having a smooth fine mesh while the right side plot has a fine mesh within 40 µm and for the outer area beyond this box it has been freely meshed. Both SD and CWD are applied.

Our numerical experiments show that a big jump in element size distribution over space may cause a sort of positive feedback effect and form nonphysical branching especially when the electric field is extremely divergent (which is the case in applied voltages with higher peaks and smaller rise-times). Such big jumps create small numerical perturbations that grow due to a SD accumulative effect in our model. Figure 7 conceptually compares different cases of element size change over space and spatial disturbances that they may produce. Part (a) of Fig. 7 shows a critical case in which a big jump can produce

disturbances that form large enough deflections on the electric field lines to add an excessive SD, and consequently deflect the main axial steamer branch. An example of this case can be seen in Fig. 4. Excessive SD in the off-axis (radial) direction deflects the streamer and accumulates charge off the axis of symmetry. Such big jumps in mesh density must be avoided if the non-physical "radial bump" has to be eliminated from the results. Part (b) shows minor disturbances that can form off-axis instability, however, they are not large enough to deflect the main axial steamer branch. An example of this case can be seen in the right side of the Fig. 6. The problem with this approach is that the number of elements is too high which leads to a long simulation time. Part (c) of Fig. 7 shows one of the possible options to minimize the effect of spatial disturbances due to element size alteration. It seems that a gradual rise in element size is the optimum approach to keep accuracy high enough and decrease the number of elements at the same time. This approach can be realized by determining an appropriate "element growth rate" in COMSOL Multiphysics meshing section. Considering the fact that SD adds artificial diffusion in the streamline direction (electric field or particle velocity), these numerical results can be explained as a keen sensitivity of SD to spatial disturbances that are caused by sudden large changes in element sizes over space.

A full three-dimensional electro-hydrodynamic model based on Eqs. (1)-(8) is also developed to study the branching dynamics of positive streamers propagating in transformer oil, since the two-dimensional axisymmetric model is not able to incorporate nonsymmetrical elements of the streamer. Streamers branches can develop when the volume charge layer ahead of the streamer head is much thinner than the streamer head radius of curvature. For an elongating streamer head with a finite radius of curvature, an infinitesimally small perturbation (but nonzero) is sufficient to trigger a self-sustaining nonlinear branching structure. Due to the strongly nonlinear nature of streamer dynamics, small fluctuations can be amplified by strong electric fields and significantly alter the propagation path of a streamer.

As a sanity check, we have studied the effect of symmetric perturbations on the streamer branching. If the mesh is fine enough to avoid misinterpreting numerical artifacts as streamer branches, the branching must be symmetric also. Then we have applied a vast variety of inhomogeneous initial conditions and perturbations to study the branching. The qualitative shape of the streamer tree, numbers and diameters of the branches and their velocities are clearly sensitive to the applied voltage and the extent of the nonsymmetrical inhomogeneities. For the same inhomogeneity, number of the branches in a positive streamer is determined by the applied voltage peak, while at the same applied voltage peak, the average diameter of branches is determined by both applied voltage rise-time and peak voltages as shown in Fig. 8.

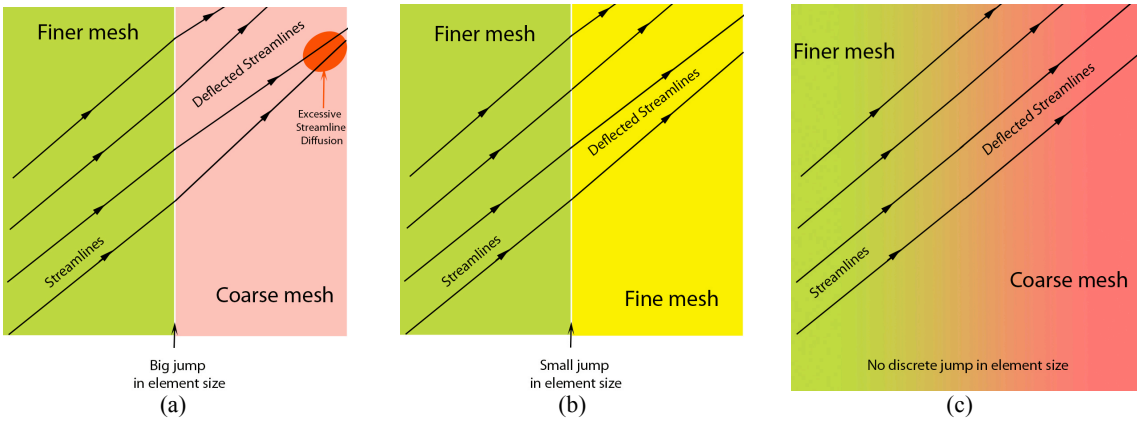

Figure 7. Different cases of element size transformation over space and spatial disturbances that they may produce, (a): critical disturbance over a big jump in element size; (b): negligible disturbance over a small jump in element size; (c): a gradual rise in element size minimizes the effect of numerical disturbances due to element size variation.

We have examined water drops and air bubbles (with higher and lower permittivities than oil, respectively), and conductive and nonconductive dust particles as macroscopic perturbations. In addition, spatial variation of oil molecule composition/density (e.g., due to locally increased temperature) and inhomogeneous initial electron density (due to external radiation sources or previous discharges) is investigated as microscopic fluctuations. The average magnitude of the perturbations is set to the minimum value required for branching. From the numerical simulation point of view there are a few interesting points in the 3D simulations. First, predefined plasma mesh in COMSOL Multiphysics greatly accelerates the model solution compared to the other types of meshing with the same meshing scheme. Second, the CWD cannot be avoided in the 3D simulations due to the convergence issues.

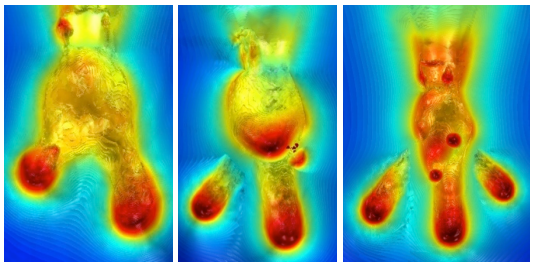

(a) (b) (c)

Figure 8. Streamer stochastic branching caused by microscopic perturbations distributed by a normal Gaussian function. Electric field distributions a few tens of nanoseconds after the streamer head branches out under applied impulse voltages with (a): 200 kV peak, (b): 250 kV peak, (c): 350 kV peak, all with 10 ns rise-time.

5. References

1. IEC Standard #60897, "Methods for the determination of the lightning impulse breakdown voltage of insulating liquids."
2. Needle-sphere transformer oil breakdown experimental setup at ABB Corporate Research, Västerås, Sweden. Courtesy of Rongsheng Liu.
3. Reference guide, COMSOL Multiphysics 3.5a.
4. Reference guide, COMSOL Multiphysics 4.3.
5. R. Codina, "A discontinuity-capturing cross-wind-dissipation for the finite element solution of the convection-diffusion equation," *Comp. Methods in Appl. Mech. and Eng.,* **110**, pp. 325-342 (1993)
6. F. O'Sullivan, "A model for the initiation and propagation of electrical streamers in transformer oil and transformer oil based nanofluids," *Ph.D. dissertation, Massachusetts Institute of Technology*, Cambridge, MA, USA (2007)
7. J. G. Hwang, "Elucidating the mechanisms behind pre-breakdown phenomena in transformer oil systems," *Ph.D. dissertation, Massachusetts Institute of Technology*, Cambridge, MA, USA (2010)
8. J. Jadidian, M. Zahn, N. Lavesson, O. Widlund, K. Borg, "Effects of Impulse Voltage Polarity, Peak Amplitude and Rise-Time on Streamers Initiated from a Needle Electrode in Transformer Oil," *IEEE Transactions on Plasma Science*, **40**, pp. 909 – 918 (2012)
9. J. Jadidian, M. Zahn, N. Lavesson, O. Widlund, K. Borg, "Impulse breakdown delay in liquid dielectrics," *Applied Physics Letters*, **100**, 192910 (2012)
10. J. Jadidian, M. Zahn, N. Lavesson, O. Widlund, K. Borg, "Surface Flashover Breakdown Mechanisms on Liquid Immersed Dielectrics," *Applied Physics Letters*, **100**, 172903 (2012)
11. C. Zener, "A theory of the electrical breakdown of solid dielectrics," *Proc. Roy. Soc. A*, pp. 523-529 (1934)
12. IEC Standard # 60060-1, "High-voltage test techniques - Part 1: General definitions and test requirements."

6. Acknowledgements

This work has been supported by ABB Corporate Research, Västerås, Sweden, and IEEE Dielectrics and Electrical Insulation Society.